

Computational Study of NACA 0012 Airfoil in Air-Sand Particle Two-Phase Flow at Reynolds Number of $Re=1.76 \times 10^6$

Dimitra C. Douvi, Eleni C. Douvi, Dionissios P. Margaritis

Abstract—The current study deals with numerical simulations of a National Advisory Committee of Aeronautics (NACA) airfoil, NACA 0012, using a commercial Computational Fluid Dynamics (CFD) Code, in air phase flow as well as in two-phase flow of air and sand particles, which consisted of 1 percent and 5 percent sand particles in air. The simulations were accomplished for Reynolds number of $Re=1.76 \times 10^6$, at various angles of attack, on Realizable $k-\epsilon$ turbulence model and the injection of the particles was succeeded using the Discrete Phase Model (DPM). The validation of the obtained numerical results was achieved by comparing them with reliable experimental data from other researchers and it was shown that the existence of sand particles in the air influences the aerodynamic performance of the airfoil. In particular, the predicted lift coefficient was decreased and at the same time the drag coefficient was increased. By the help of contours of static pressure and DPM concentration, it was possible to study the region around NACA 0012 airfoil.

Index Terms—aerodynamic performance, airfoil, CFD code, air-sand particles two-phase flow.

I. INTRODUCTION

In the few last years, many computational studies were performed aiming to the aerodynamic behavior of an airfoil-shaped body moving through the air. Nowadays complex multiphase flow problems, like an air-solid particle two-phase flow problem, can be solved by the help of CFD, in order to study the influences of secondary phases on the aerodynamic behavior of an airfoil and to pursue optimal aerodynamic performance.

To begin with, in 2018, an interesting CFD study was conducted by Han et al. [1] in order to find out how erosion and contamination at the foremost edge of blade tip airfoil, in other words the leading edge, for a wind turbine is possible to affect its Annual Energy Production (AEP). They showed that the AEP can be reduced by 2%–3.7%, accordingly the severity of these conditions.

Next, one of the first computational studies was conducted by Kamura et al. [2], who used a wall function in order to take into account the airfoil surface roughness due to sand erosion. They showed the change of the airfoil geometry and flow field with proceeding the erosion for various wall materials.

Dimitra C. Douvi, Mechanical Engineering and Aeronautics Department, University of Patras, Patras, Greece

Eleni C. Douvi, Mechanical Engineering and Aeronautics Department, University of Patras, Patras, Greece

Dionissios P. Margaritis, Mechanical Engineering and Aeronautics Department, University of Patras, Patras, Greece

Some years later, Khakpour et al. [3] studied the effects of ratio of sand to air mass flow rate, sand dimensions and sand/air drift velocity by developing mathematical formulations for air, which is the continuum phase, and the sand particles, i.e. the discrete phase.

Another interesting approach has been proposed by Knopp et al. [4] who proposed a new method, based on the approach of equivalent sand grain, for the prediction of the aerodynamic effects of an airfoil surface roughness by extending the $k-\omega$ turbulence models. In 2013, Salem et al. [5] developed a CFD model, based on the Navier-Stokes equations and the SST $k-\omega$ turbulence model, combined with an accumulation model in order to predict wind turbine blades performance degradation in environments with dust.

Much research regarding the simulation of the particles flow over an airfoil has also been conducted by Diab et al. [6]. They compared the contamination susceptibility of different airfoil types and they concluded that under dusty conditions, the airfoil types that perform better are these with low surface contamination sensitivity. In 2016, El-Din and Diab [7] concentrated on the study of wind turbine blade erosion in dusty environment, by developing a model of an airfoil forced to sand blasting which led to airfoil erosion, using a CFD Code along with an erosion model, and they suggest that the developed model can be used to predict the power deterioration of eroded blades.

In 2017, Zidane et al. [8] investigated numerically the wind turbine blade performance in dusty air flow, using the Transition SST turbulence model and the Discrete Phase Model under different sand particles flow rates, and it was resulted that this method can estimate accurately sand particles impact on wind turbine blades.

As regards the impact of the Reynolds number on the aerodynamic performance of an airfoil, Qu et al. [9] showed numerically and experimentally that the changes on the aerodynamic coefficients of the airfoil are getting smoother and smaller as the Reynolds number increases.

In our previous work [10], we studied the aerodynamic behavior of a NREL S809 airfoil operating at Reynolds numbers of $Re=1 \times 10^6$ and $Re=2 \times 10^6$ in an air-sand particle two-phase flow, for two different concentrations of sand particles in the air, i.e. 1% and 10%, using the realizable $k-\epsilon$ and SST $k-\omega$ turbulence models. Now, in this study, the aim is to investigate the aerodynamic behavior of a different airfoil type, NACA 0012 airfoil, in air phase flow and in air-sand particle two-phase flow consisted of 1% and 5% sand particles in air, using a commercial CFD code, at

$Re=1.76 \times 10^6$, using the most appropriate turbulence model, which is the realizable $k-\epsilon$, as it was found in previous study. The computational method as well as the calculations made in the previous study [10] were also used in the current study, that refers to a different airfoil operating under different conditions. The validation of the computational results was succeeded by comparing them with existing reliable data and it was found that sand particles in the air affect significantly the aerodynamic performance of the airfoil.

II. AIR-SAND PARTICLE TWO-PHASE FLOW OVER AN AIRFOIL

Air-sand particle two-phase flow is a discrete phase flow, which is simulated by the Euler-Lagrange approach. The dispersed phase, in other words the sand particles, interacts with the continuum air phase, which means that energy, mass, and momentum of the sand particles are exchanged with the air. Particularly, only momentum is transferred from the air to the dispersed phase as regards air-sand particle two-phase flow.

In case an airfoil operates in a discrete air-sand particle two-phase flow field, the aerodynamic performance of the airfoil is degraded. Specifically, the pressure gradient, the boundary layer, and the shear stress factor can be affected by the presence of sand particles. As a result, the lift force decreases while the drag force increases, because of the change in momentum due to the particles that reflect on the airfoil surface.

III. COMPUTATIONAL METHOD

A. Computational Mesh

Before the computational study, the NACA 0012 airfoil, which is a symmetrical airfoil as thick as the 12% of the chord length without camber, was designed to the geometry system, and then a structured C-mesh domain of 80,000 cells, as was found to be the most suitable after a grid independence study conduction, was created in mesh component system around the airfoil.

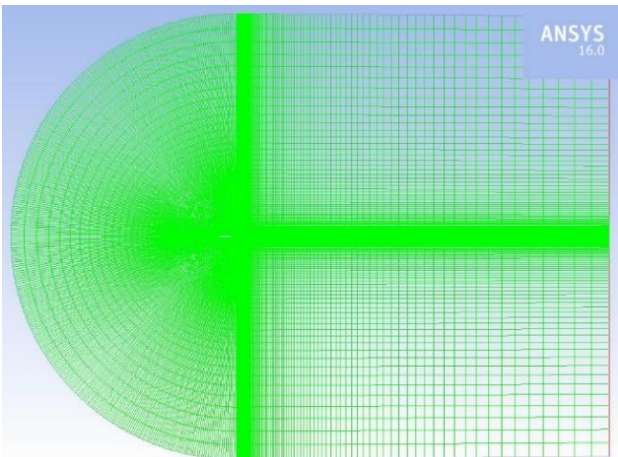


Fig. 1. Structured C-mesh domain.

Notably, the height of the C-mesh domain was set to be equal to 25 chord lengths, and the mesh is denser close to the airfoil, resulting at a value of the maximum $y^+=0.2$, in order to resolve appropriately the boundary layer. The mesh around the airfoil and the C-mesh domain, are illustrated in Fig. 1

and Fig. 2 respectively.

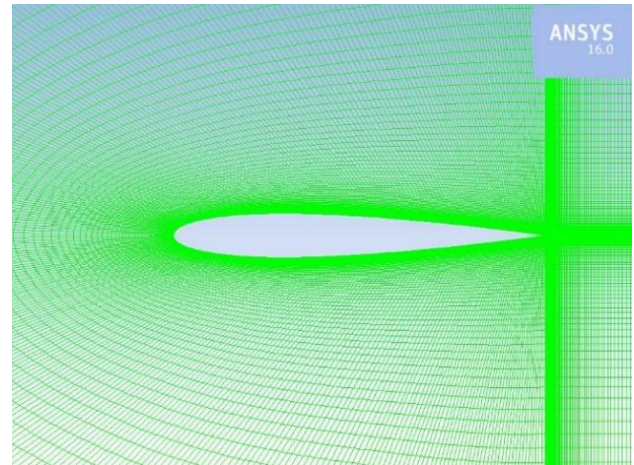


Fig. 2. The mesh close to the NACA 0012 airfoil.

B. Realizable $k-\epsilon$ Turbulence Model

The computational study was accomplished by the help of a commercial CFD Code, ANSYS Fluent 16 [11], which solves conservation equations for momentum, mass, and supplementary transport equations for turbulent flows. The study of the air-sand particle two-phase flow over a NACA 0012 airfoil is accomplished via the Lagrangian Discrete Phase Model (DPM). The Navier–Stokes equations solve the continuum air phase, while many spherical sand particles are tracked into the computational domain.

In ANSYS Fluent 16 [11], the change in momentum of a sand particle through each control volume is calculated by the equation:

$$F = \sum \left(\frac{18\mu C_D Re}{\rho_p d_p^2 24} (u_p - u) + F_{other} \right) \dot{m}_p \Delta t \quad (1)$$

where μ is the viscosity of the fluid, C_D the drag coefficient, Re the relative Reynolds number, ρ_p the density of the particle, d_p the diameter of the particle, u_p the velocity of the particle, u the velocity of the fluid, F_{other} other interaction forces, \dot{m}_p the particles mass flow rate and Δt the size of the time step.

The prediction of the path line of each discrete phase sand particle is accomplished by the integration of the force balance on the particle. The particle inertia is equal to the forces acting on the particle. This equality in horizontal axis, given the drag force per unit particle mass, $F_D(\bar{u} - \bar{u}_p)$, and an additional acceleration term, \bar{F} , also force per unit particle mass, can be written as:

$$\frac{du_p}{dt} = F_D(\bar{u} - \bar{u}_p) + \frac{\bar{g}}{\rho_p}(\rho_p - \rho) + \bar{F} \quad (2)$$

and

$$F_D = \frac{18\mu C_D Re}{\rho_p d_p^2 24} \quad (3)$$

where \bar{u} is the velocity of the fluid phase, \bar{u}_p is the velocity and ρ_p is the density of the particle, ρ is the density and μ is the molecular viscosity of the fluid, d_p is the particle

diameter and Re is the relative Reynolds number, which is described by the equation:

$$Re \equiv \frac{\rho d_p |\vec{u}_p - \vec{u}|}{\mu} \quad (4)$$

The simulations were conducted at $Re=1.76 \times 10^6$, therefore the flow can be described as incompressible as well as turbulent, for various angles of attack ranging from -9 to 16 degrees, similarly as in previous study [10]. Since the flow is turbulent, the realizable $k-\epsilon$ turbulence model, that was suggested by Shih et al. [12], was chosen for the simulations, because not only it is appropriate for aerodynamic applications but also it cooperates well with Discrete Phase Model (DPM). Particles damp and product turbulence eddies, which are included in the calculations by enabling two-way turbulence coupling.

First of all, the steady one-phase air flow around the airfoil was studied and compared to reliable data predicted by XFOIL [13], in order to be validated. Then the study of the steady discrete air-sand particle two-phase flow, consisted of 1% and 5% of spherical sand particles with diameter 0.5 mm and density equal to 2196.06 kg/m^3 in the air flow, was conducted via the DPM.

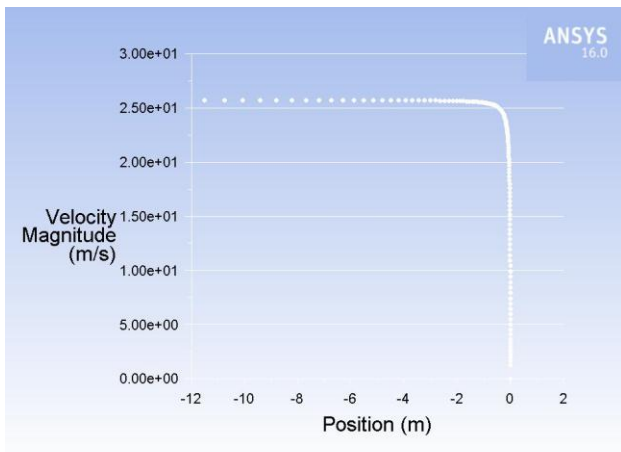


Fig. 3. Velocity magnitude from velocity inlet to leading edge of the airfoil.

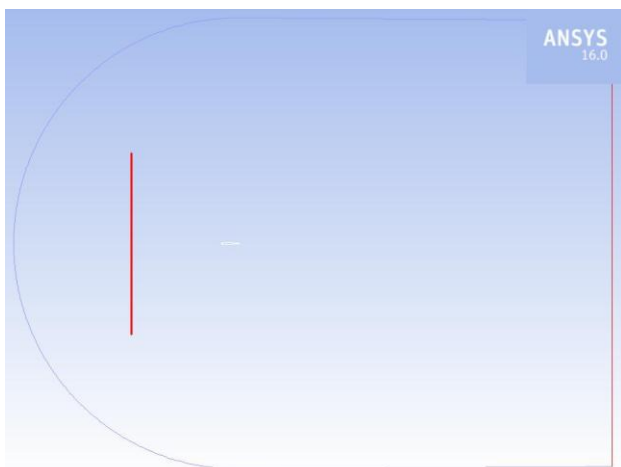


Fig. 4. The particles injection location.

The computational method used for the air-sand particle two-phase flow is the same with the methodology that was used in our previous study [10]. The injection of the particles was set at the minimum distance upstream the NACA 0012

airfoil where the flow is undisturbed, as shown in Fig. 3 and in Fig. 4, which leads to a simplified solution and less computational time. Notably, the horizontal axis velocity is equal to air velocity and the vertical axis velocity, calculated by the approach method, depends on the diameter of the particles. Finally, the emerged two-phase flow results were compared to the one-phase flow results in order to show the impact of the sand particles on the aerodynamic performance of NACA 0012 airfoil.

IV. RESULTS AND DISCUSSION

Computational study of the air flow and of the two-phase flow over NACA 0012 airfoil was conducted at $Re=1.76 \times 10^6$ at various angles of attack.

A. Aerodynamic Coefficients

The aerodynamic coefficients were calculated by the realizable $k-\epsilon$ turbulence model, and then compared with reliable XFOIL predicted data [13] concerning the one-phase air flow over the NACA 0012 airfoil.

Fig. 5 depicts the computational results of the lift coefficient for the NACA 0012 airfoil versus the angle of attack at $Re=1.76 \times 10^6$ for air flow and two-phase flows consisted of 1% and 5% sand particles in the air compared with one-phase air flow reliable data. It is shown that the predicted lift coefficient curves increase linearly with the angle of attack and there is a good agreement with the XFOIL data for small angles of attack, while there is a difference between the computational results and the XFOIL data for angles of attack higher than 14 degrees, due to stall conditions. Besides, the impact of sand concentration is obvious, and more specifically as the concentration of sand particles in the air increases, a greater degradation of the lift coefficient is observed.

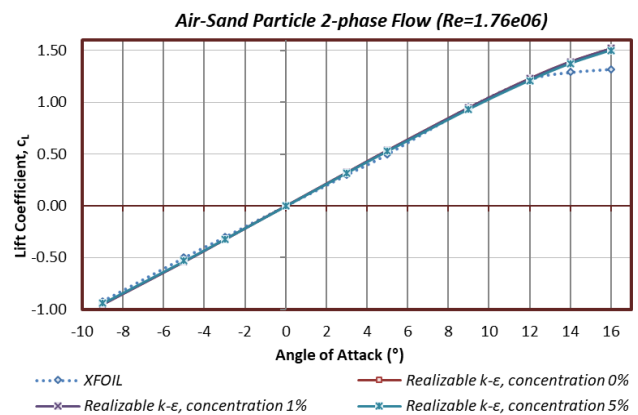


Fig. 5. Comparison between XFOIL reliable data and simulation results of the lift coefficient curve for a NACA 0012 airfoil for realizable $k-\epsilon$ turbulence model at $Re=1.76 \times 10^6$ for one-phase and two-phase flows consisting of 1% and 5% sand particles in the air.

In Fig. 6 is given more clearly the percentage of lift coefficient degradation due to the presence of sand particles in the air for the NACA 0012 airfoil at Reynolds number $Re=1.76 \times 10^6$ versus the angle of attack. The maximum lift coefficient degradation was found to be -2.4% at 3 degrees angle of attack for 1% sand particles in the air, while for 5% concentration of sand particles in the air the maximum

degradation was -0.5% at 3 and at 5 degrees angle of attack.

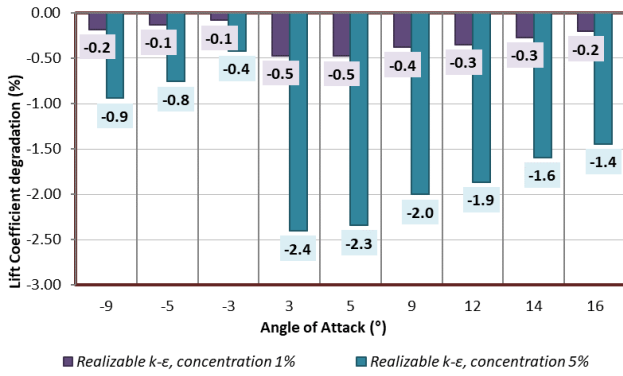


Fig. 6. Percentage of lift coefficient degradation for a NACA 0012 airfoil due to presence of sand particles in the air.

Fig. 7 illustrates the computational results of the drag coefficient versus the angle of attack at $Re=1.76 \times 10^6$. It is observed that the predicted drag coefficient values are higher than the data by other researchers for a wide range of angles of attack due to the inability of the realizable k-ε turbulence model to predict exactly the transition of boundary layer from laminar to turbulent. Moreover, an upward translation of the drag coefficient curve is caused by the presence of sand particles in the air, which leads to larger skin frictional drag. This upward translation is more noticeable for 5% concentration of sand particles in the air flow.

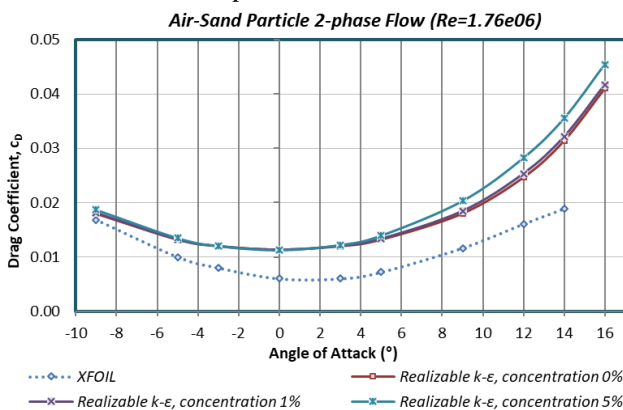


Fig. 7. Comparison between XFOIL reliable data and simulation results of the drag coefficient curve for a NACA 0012 airfoil for realizable k-ε turbulence model at $Re=1.76 \times 10^6$ for one-phase and two-phase flows consisting of 1% and 5% sand particles in the air.

In Fig. 8 is presented the percentage of drag coefficient increase due to the presence of sand particles in the air for the NACA 0012 airfoil versus the angle of attack. The maximum increase of the drag coefficient is shown at 12 degrees angle of attack and is equal to 2.8% for 1% sand particles in the air, and 14.6% also at 12 degrees angle of attack for the higher concentration of sand particles in the air.

Next, Fig. 9 presents the power coefficient curve for a three-bladed horizontal axis wind turbine which blades are constructed by the NACA 0012 airfoil profile versus the twist angle of the blade at Reynolds number of $Re=1.76 \times 10^6$. The power coefficient was predicted by the help of the empirical Wilson equation [14] taking into account the aerodynamic performance of the blade airfoil, the number of blades and the

tip speed ratio, for one-phase and two-phase flows. It is observed that the presence of sand particles in the air results to a decreased power coefficient of a three-bladed wind turbine. This decrease can change the Annual Energy Production (AEP) of wind turbines in a long term. In Fig. 10 the percentage of power coefficient degradation is given more clearly. It seems that as the twist angle as well as the concentration of sand particles in the air increase, the degradation of the wind turbine power coefficient is greater.

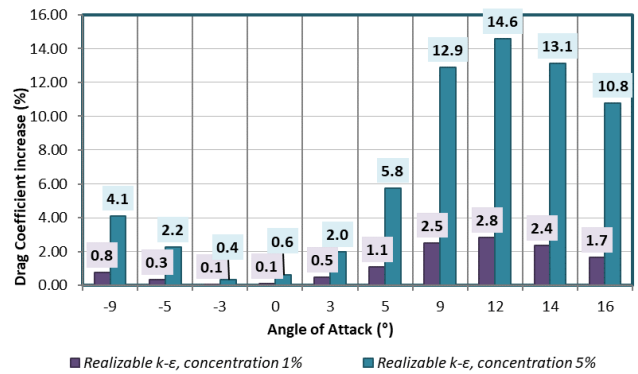


Fig. 8. Percentage of drag coefficient increase for a NACA 0012 airfoil due to presence of sand particles in the air.

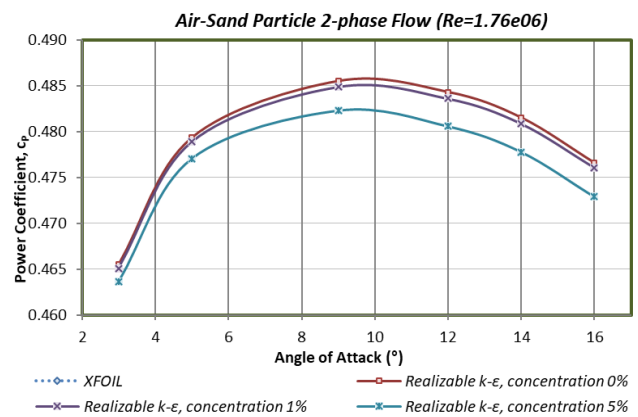


Fig. 9. Comparison between reliable data provided by other researchers and simulation results of the power coefficient curve for a three-bladed horizontal axis wind turbine for realizable k-ε turbulence model at $Re=1.76 \times 10^6$ for one-phase and two-phase flows consisting of 1% and 5% sand particles in the air.

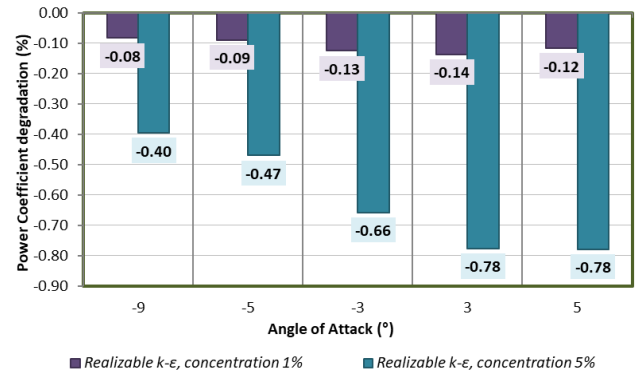
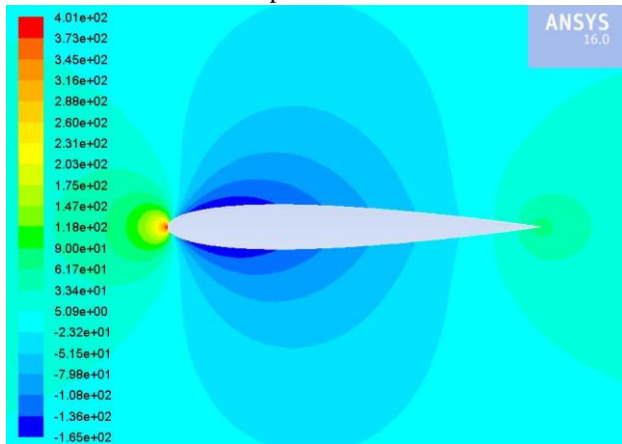


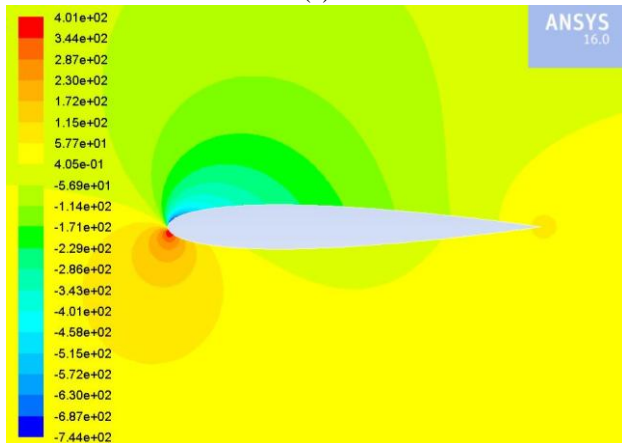
Fig. 10. Percentage of power coefficient degradation for a three-bladed horizontal axis wind turbine at $Re=1.76 \times 10^6$ due to presence of sand particles in the air.

B. Contours of Static Pressure

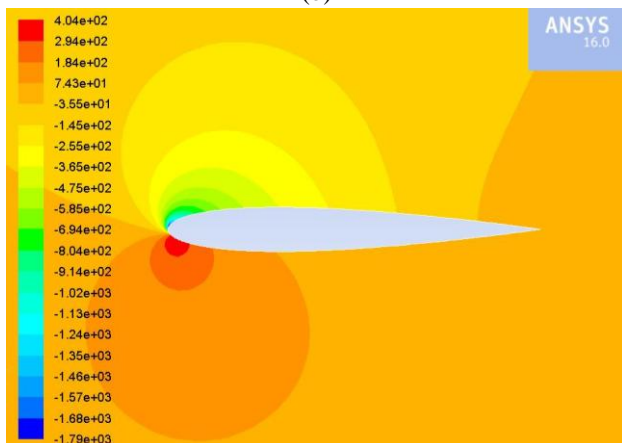
Following, Fig. 11, Fig. 12 Fig. 13 illustrate the region around the NACA 0012 airfoil using contours of static pressure at angles of attack equal to 0°, 5° and 9°, and at $Re=1.76 \times 10^6$ with the realizable $k-\epsilon$ model for air flow and for air-sand particle two-phase flows consisting of 1% and 5% concentration of sand particles in the air.



(a)



(b)

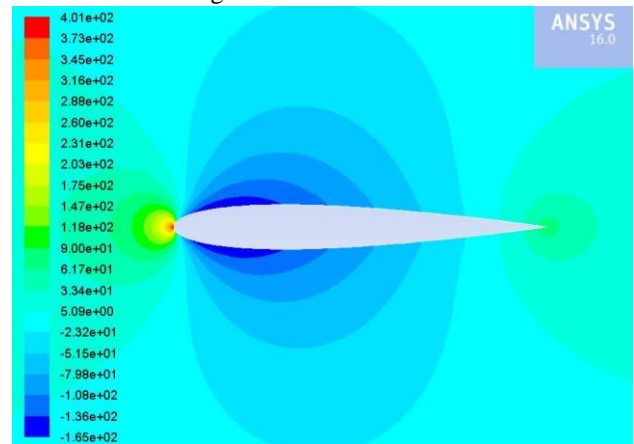


(c)

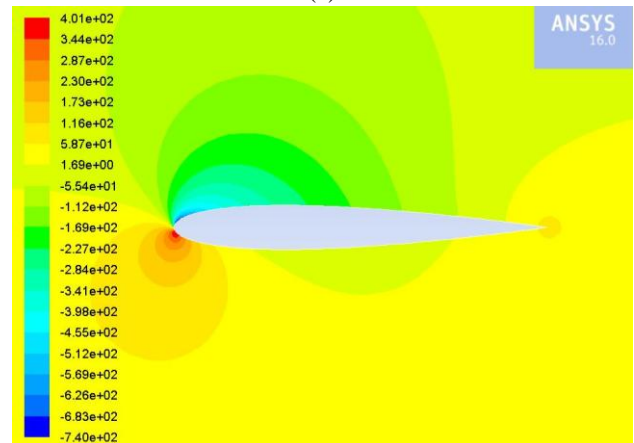
Fig. 11. Contours of static pressure at (a) 0°, (b) 5° and (c) 9° angles of attack at $Re=1.76 \times 10^6$ with the realizable $k-\epsilon$ turbulence model for a NACA 0012 airfoil for air flow.

Fig. 11 depicts the contours of static pressure at various angles of attack for a NACA 0012 airfoil for air flow. The stagnation points, where the static pressure is equal to the total, are obvious. As the angle of attack increases it is observed that the leading-edge stagnation point moves

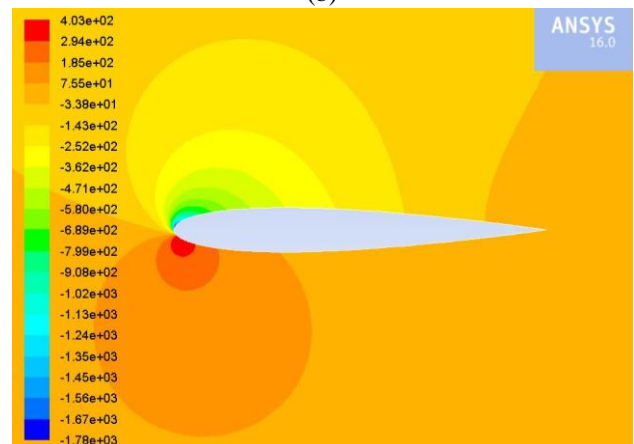
towards to the trailing-edge on the lower surface of the airfoil and the trailing-edge stagnation point seems to move forward the leading edge. Moreover, the pressure achieves higher values on the lower surface of the airfoil than the pressure of the flow resulting on an effective upward pushed of the airfoil normal to the incoming flow stream and a higher lift coefficient as the angle of attack increases.



(a)



(b)

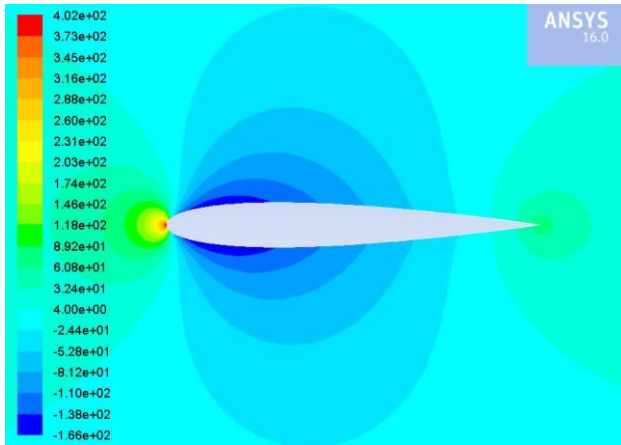


(c)

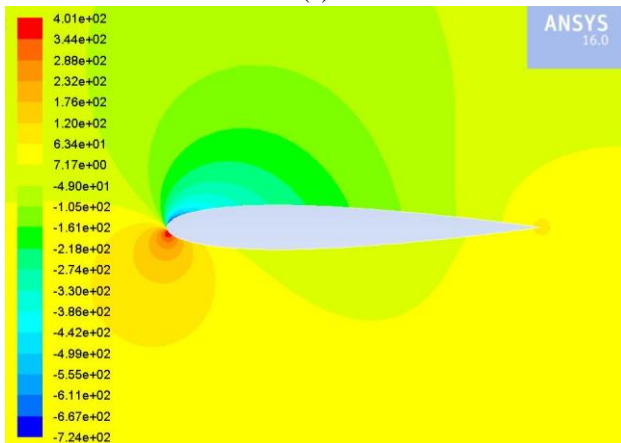
Fig. 12. Contours of static pressure at (a) 0°, (b) 5° and (c) 9° angles of attack at $Re=1.76 \times 10^6$ with the realizable $k-\epsilon$ turbulence model for a NACA 0012 airfoil for air-sand particle two-phase flow and 1% concentration of sand particles in the air.

Regarding the static pressure contours for air-sand particle two-phase flows, there is a very little difference between them and the corresponding contours in one-phase air flow, as can be seen in Fig. 12 and Fig. 13. More specifically, these

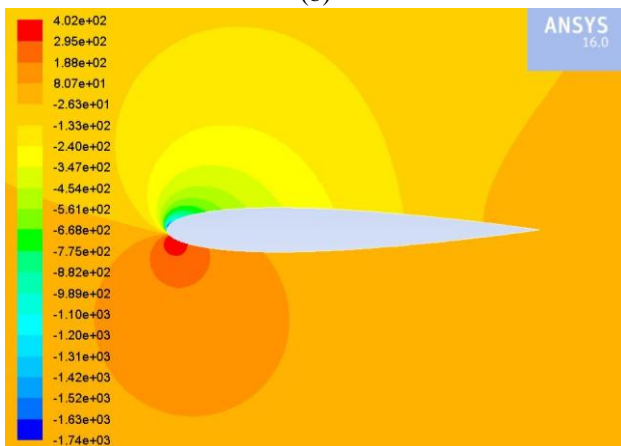
differences are observed, especially in the case of 5% concentration of sand particles in the air, on the greater pressure values on the upper surface and on the lower values on the lower surface of the airfoil, but the aerodynamic behavior of the airfoils still seems to be similar at the same angles of attack. In the case of 1% concentration of sand particles in the air, the differences are minor.



(a)



(b)



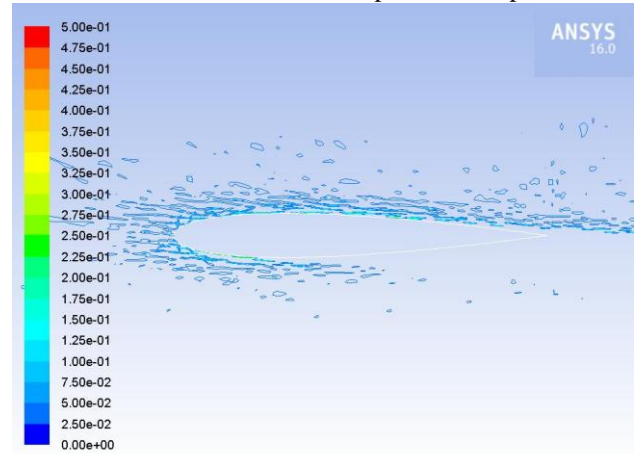
(c)

Fig. 13. Contours of static pressure at (a) 0° , (b) 5° and (c) 9° angles of attack at $Re=1.76 \times 10^6$ with the realizable $k-\epsilon$ turbulence model for a NACA 0012 airfoil for air-sand particle two-phase flow and 5% concentration of sand particles in the air.

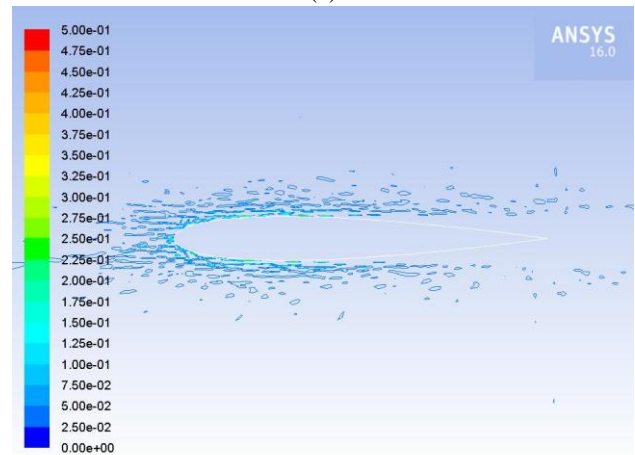
C. Contours of DPM Concentration

Finally, in Fig. 14 and Fig. 15 are given the contours of DPM concentration over the NACA 0012 airfoil at various

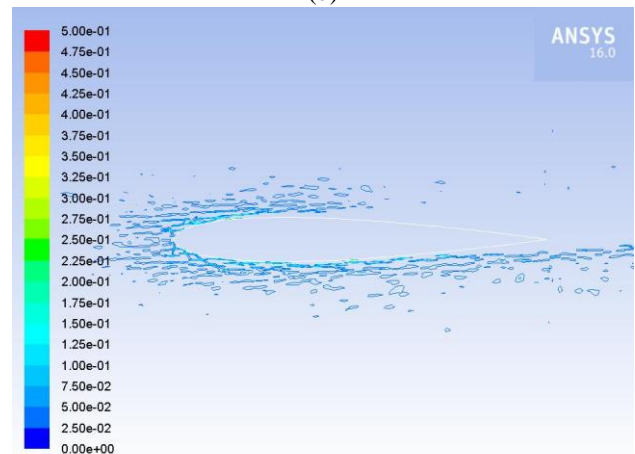
angles of attack at $Re=1.76 \times 10^6$ with the realizable $k-\epsilon$ turbulence model for both air-sand particle two-phase flows.



(a)



(b)



(c)

Fig. 14. Contours of DPM concentration at (a) 0° , (b) 5° and (c) 9° angles of attack at $Re=1.76 \times 10^6$ with the realizable $k-\epsilon$ turbulence model for a NACA 0012 airfoil for air-sand particle two-phase flow and 1% concentration of sand particles in the air.

It is apparent that sand particles concentrate mostly in the region of the leading-edge to the middle of the lower surface of the airfoil, as well as on the upper surface of the airfoil for small angles of attack. As the angle of attack increases, sand particles concentrate in the regions of the leading-edge to the middle of the upper and to the middle of the lower surfaces of the airfoil. Also, as the concentration of sand particles in the

air increases, the particles surrounding the airfoil are more.

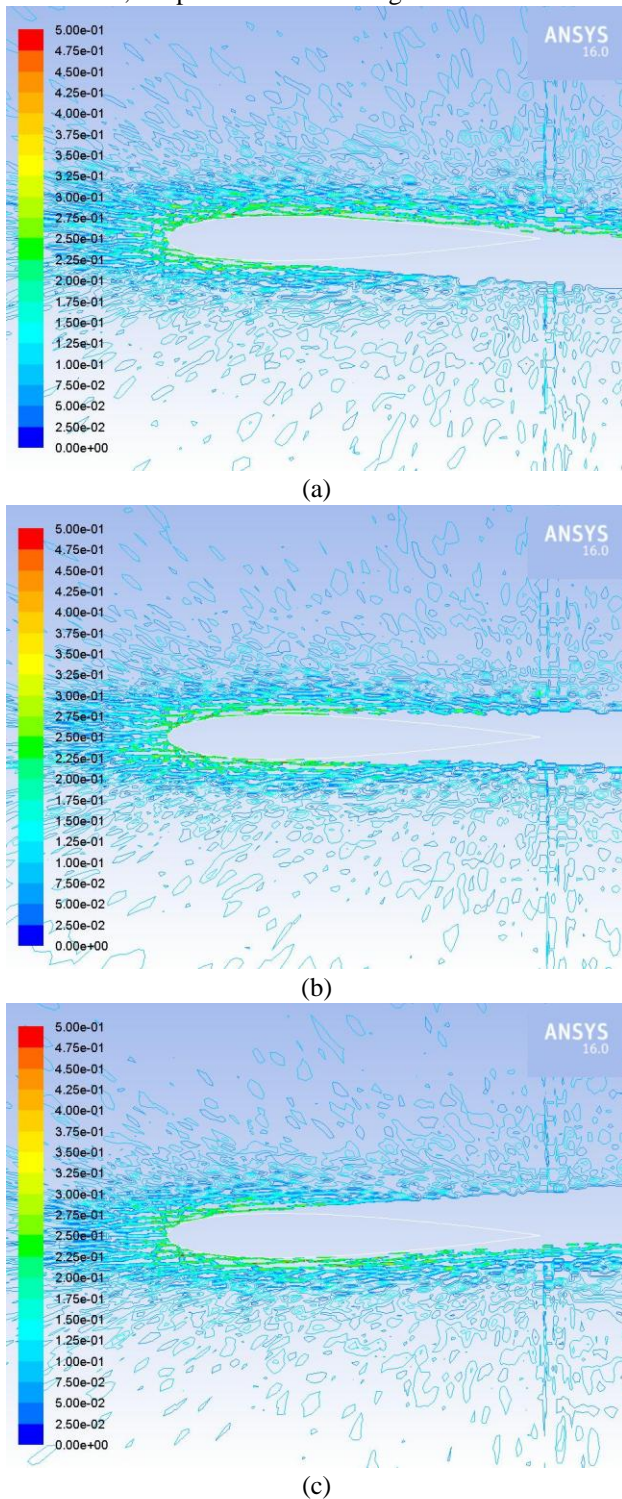


Fig. 15. Contours of DPM concentration at (a) 0°, (b) 5° and (c) 9° angles of attack at $Re=1.76 \times 10^6$ with the realizable $k-\epsilon$ turbulence model for a NACA 0012 airfoil for air-sand particle two-phase flow and 1% concentration of sand particles in the air.

V. CONCLUSION

The present study set out to confirm the impact of air-sand particle two-phase flow, consisted of 1 and 5 percent sand particles in the air, on the aerodynamic performance of NACA 0012 airfoil at $Re=1.76 \times 10^6$ using the realizable $k-\epsilon$ turbulence model.

Summing up the results, it can be concluded that the

concentration of sand particles in the air affects the aerodynamic performance of NACA 0012 airfoil, since a degradation of lift coefficient as well as an increase of drag coefficient are observed for a wide range of angles of attack compared to one-phase air flow data provided by other researchers, for both concentrations of sand particles in the air.

Specifically, as regards the lift coefficient curves, they increase linearly with the angle of attack and there is a good agreement between the predicted values and the data provided by other researchers especially for small angles of attack. The predicted drag coefficient values are higher than the data by other researchers, while two-phase flow drag coefficient curves are translated upwards.

Next, the prediction of the power coefficient of a three-bladed horizontal axis wind turbine which blades are constructed by the NACA 0012 airfoil profile at $Re=1.76 \times 10^6$ showed that the presence of particles in the air causes a decreased power coefficient, which depends on the twist angle and on the presence of sand particles in the air.

Additionally, based on the observation of the region around NACA 0012 airfoil using contours of static pressure, it has been shown that the leading-edge stagnation point is moving towards to the trailing-edge on the lower surface of the airfoil as the angle of attack increases, and also the trailing-edge stagnation point moves forward on the airfoil.

Furthermore, the static pressure achieves higher values on the lower surface of the airfoil than the pressure of the flow, resulting to an effective upward pushed of the airfoil normal to the incoming flow stream, and as the angle of attack increases the lift coefficient gets higher.

In air-sand particle two-phase flow it has been shown that close to the trailing-edge and on the lower surface of the airfoil some more differences between one-phase and two-phase results are detected. Regarding the static pressure contours, pressure values on the upper surface of the airfoil are greater while values on the lower surface are lower. Nevertheless, the pressure distribution of the airfoil seems to be similar in both one phase and the two cases of two-phase flows and at the same angles of attack.

Finally, contours of sand particles concentration over NACA 0012 airfoil suggest that particles seem to concentrate mainly on the upper surface and in the region of the leading-edge to the middle of the lower surface of the airfoil for small angles of attack. As the angle of attack increases, particles concentrate on a smaller region of the airfoil, while the increasing concentration of the particles in the air flow is obvious.

REFERENCES

- [1] W. Han, J. Kim, and B. Kim. (2018, Jan.). Effects of contamination and erosion at the leading edge of blade tip airfoils on the annual energy production of wind turbines. *J. Renewable Energy*. 115, pp. 817-823. Available: <https://doi.org/10.1016/j.renene.2017.09.002>.
- [2] K. Kamura, K. Toda, and M. Yamamoto, "Numerical simulation of performance change of airfoil due to sand erosion." *J. Nihon Kikai Gakkai Ronbunshu, B Hen/Transactions of the Japan Society of Mechanical Engineers*, vol. 67(662), Oct. 2001, pp. 2397-2404. Available: <https://doi.org/10.1299/kikaib.67.2397>.
- [3] Y. Khakpour, S. Bardakji, and S. Nair, "Aerodynamic Performance of Wind Turbine Blades in Dusty Environments," *ASME International Mechanical Engineering Congress and Exposition Conf. USA*, 2008.

- [4] T. Knopp, B. Eisfeld, and J. B. Calvo, "A new extension for $k-\omega$ turbulence models to account for wall roughness," *Int. J. of Heat and Fluid Flow*, vol. 30, Feb. 2009, pp. 54-65 Available: <https://doi.org/10.1016/j.ijheatfluidflow.2008.09.009>.
- [5] H. Salem, A. Diab, and Z. Ghoneim, "CFD Simulation and Analysis of Performance Degradation of Wind Turbine Blades in Dusty Environments," *Int. Conf. on Renewable Energy Research and Applications* Spain, 2013.
- [6] A. Diab, M. Alaa, A. H. El-Din, H. Salem, and Z. Ghoneim, "Performance Degradation of Wind Turbine Airfoils due to Dust Contamination: A Comparative Numerical Study," *ASME Turbo Expo 2015: Turbine Technical Conference and Exposition, GT 2015* Canada, 2015.
- [7] A. H. El-Din, and A. A. Diab, "Preliminary Study of the Blade Erosion for a Wind Turbine Operating in a Dusty Environment," *ASME Turbo Expo 2016: Turbomachinery Technical Conference and Exposition, GT 2016* South Korea, 2016.
- [8] I. F. Zidane, K. M. Saqr, G. Swadener, X. Ma, and M. F. Shehadeh. (2017, Aug.). Computational fluid dynamics study of dusty air flow over NACA 63415 airfoil for wind turbine applications. *Jurnal Teknologi*. 79, pp. 1-6. Available: <https://doi.org/10.11113/jt.v79.11877>.
- [9] H. Qu, J. Hu, and X.Gao, "The Impact of Reynolds Number on Two-Dimensional Aerodynamic Airfoil Flow," *2009 World Non-Grid-Connected Wind Power and Energy Conf.* China, 2009.
- [10] D. C. Douvi, D. P. Margaritis, and A. E. Davaris. (Feb. 2017). Aerodynamic performance of a NREL S809 airfoil in an air-sand particle two-phase flow. *J. Computation*. 5. Available: <https://doi.org/10.3390/computation5010013>.
- [11] ANSYS® (2019, March 20). Academic Research (Release 16.0) [Online]. Available: <http://www.ansys.com>
- [12] T.-H. Shih, W. W. Liou, A. Shabbir, Z. Yang, and J. Zhu. (1995, March). A new $k-\epsilon$ eddy-viscosity model for high Reynolds number turbulent flows—model development and validation. *Computers Fluids*. 24 (3), pp. 227–238. Available: [https://doi.org/10.1016/0045-7930\(94\)00032-T](https://doi.org/10.1016/0045-7930(94)00032-T).
- [13] M. Drela, *XFOIL: An Analysis and Design System for Low Reynolds Number Airfoils*. In *Low Reynolds Number Aerodynamics*. Berlin: Springer-Verlag, 1989, vol 54, pp. 1-12. Available: https://doi.org/10.1007/978-3-642-84010-4_1.
- [14] R. E. Wilson, P. B. S. Lissaman, and S. N. Walker, *Aerodynamic performance of wind turbines. Final report*. Oregon State University: Corvallis, USA, 1976.



Dimitra C. Douvi, born in Korinthos, Greece on May 31st, 1989. She is a PhD student of the Mechanical Engineering and Aeronautics Department at University of Patras. Her doctoral thesis is experimental and computational investigation of aerodynamic behavior of wind turbine rotor in multiphase flows. She is participating in 6 international conferences on the above scientific areas and has 3 publications on high-interested impact factor Journals.



Eleni C. Douvi, born in Korinthos, Greece on March 15th, 1984. She is a post-doctoral researcher of the Mechanical Engineering and Aeronautics Department at University of Patras. Her research activity is the proposal of the optimum geometry of a horizontal axis tidal turbine rotor. Her doctoral thesis was experimental and computational investigation of aerodynamic behavior of wings in heavy rain, applied to horizontal axis wind turbine blades. In her diploma thesis was dealing with the experimental study of fluid mechanics applying LDA and PDA measurements. She is participating in 13 international conferences on the above scientific areas and has 6 publications on high-interested impact factor Journals.



Dionissios P. Margaritis, born in Zakynthos island, Greece on September 28th, 1953. He is Professor in Mechanical Engineering and Aeronautics Department at the University of Patras, Patras, Greece. His research activities/fields are multiphase flows of gas-liquid-solid particles, gas-liquid two-phase flow air-lift pump performance, centrifugal and T-junction separation modeling in gas-liquid two-phase flow, experimental and theoretical investigation of hot air dehydration of agricultural products, experimental and theoretical investigation of capillary pumped loops, steady and transient flows in pipes and network and numerical simulation of centrifugal pump performance. Also he is dealing with fluid dynamics analysis of wind turbines and aerodynamic installations, aero-acoustic analysis and environmental impacts of wind turbines. He is participating in over 130 international conferences on the above scientific areas and has over 80 publications on high-interested impact factor Journals. Prof. Dionissios P. Margaritis is participating in several research projects supported by HAI, GSRT, CEC-THERMIE. Also he is member of AIAA, AHS, ASME and EUROMECH unions as well as of TCG (Technical Chamber of Greece)